Figures and figure supplements

Structural basis of phosphatidylcholine recognition by the C2–domain of cytosolic phospholipase $A_2\alpha$

Yoshinori Hirano *et al*

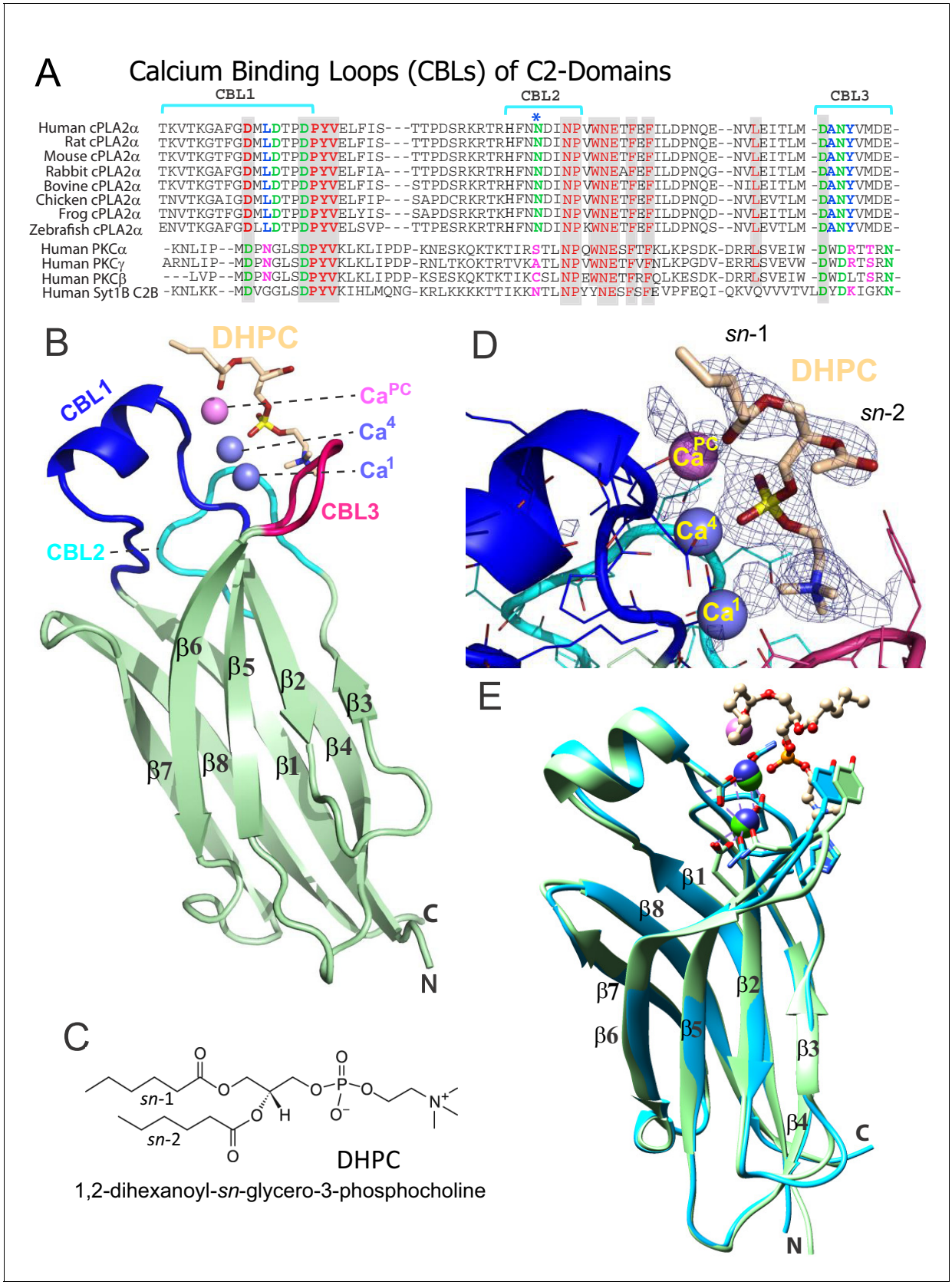

Figure 1. Structure of cPLA$_2$α C2–domain containing bound DHPC and calcium. (**A**) Sequence alignment of C2-domain calcium-binding loop (CBL) regions in cPLA2α from different eukaryotes compared to human PKCs and Syt1. Residues that bind Ca^{2+} are green. Residues interacting directly with

Figure 1 continued on next page

Figure 1 continued

PC in our structural complex (blue or blue asterisk) are absolutely conserved among eukaryotic cPLA$_2$α proteins but not in PKCs and Syt1. Conversely, residues that interact with PS in the PKCα-PS structure (magenta) are highly conserved in PKCs and Syt1, but not in cPLA$_2$α. Shaded residues are identical. The human and chicken cPLA$_2$α CBL sequences are 92% identical and 94.5% highly conserved (see ***Figure 1—figure supplement 1*** for full-length sequence alignment). (**B**) Ribbon structure representation of the cPLA$_2$α C2-domain bound to 1,2-dihexanoyl-*sn*-glycero-3-phosphocholine (DHPC). The DHPC molecule (beige stick) straddles the β1–β2 loop (CBL1, blue), β3–β4 loop (CBL2, cyan) and β5–β6 loop (CBL3, red). Ca1 and Ca4 (blue spheres) are in a similar position in the apo-form structure; whereas Ca^{PC} (magenta sphere) is unique to the DHPC-bound form. (**C**) DHPC structural formula. (**D**) *Fo-Fc* omit electron density map for the bound DHPC molecule at the 2.5σ contour level. (**E**) Superimposition of the chicken cPLA$_2$α C2-domain with bound DHPC (colored as in ***Figure 1B***) on the human lipid-free structure (PDB: 1RLW, cyan). Root mean square deviation = 0.7 Å after superimposition of Cα atoms.

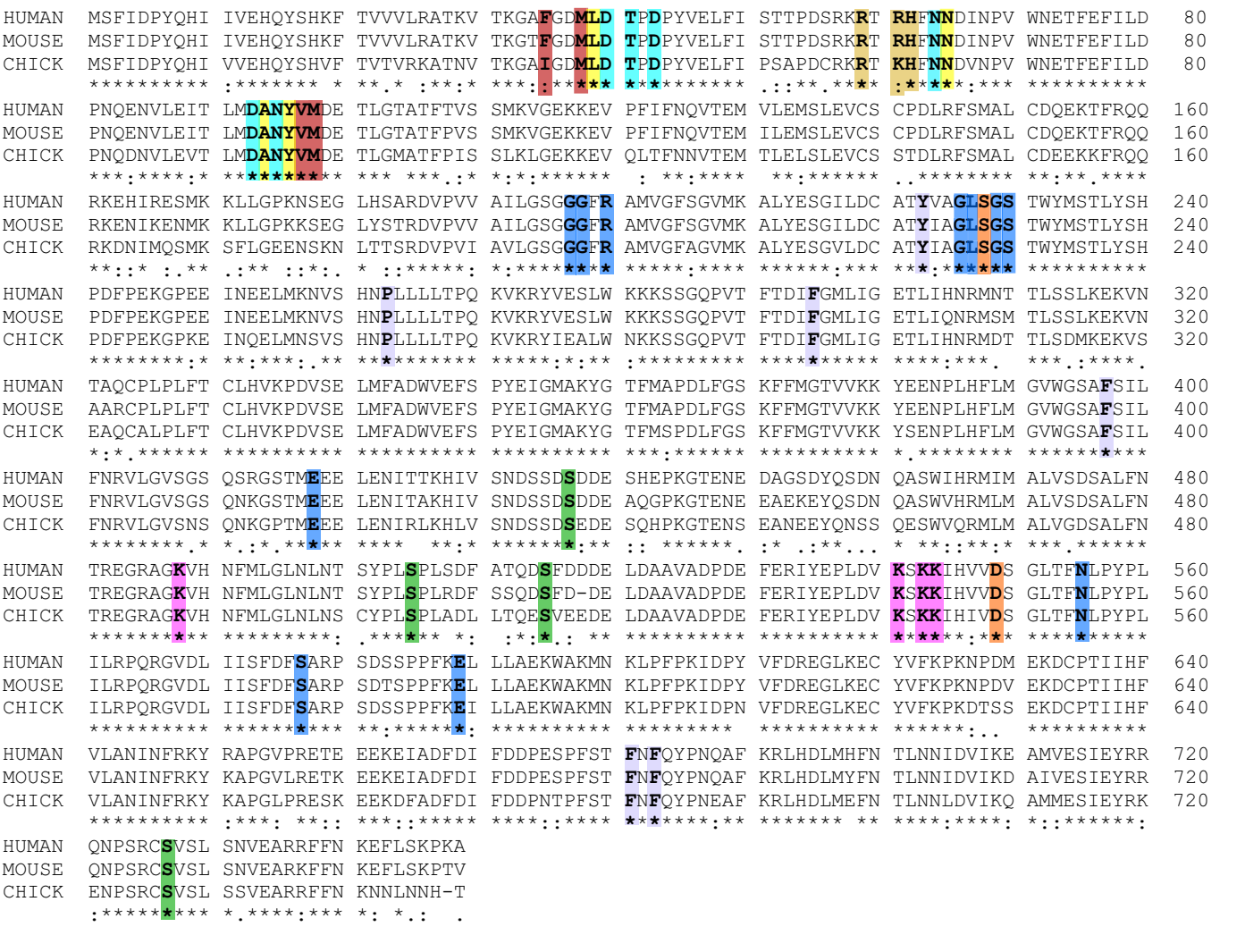

Figure 1—figure supplement 1. Sequence alignment of cPLA$_2\alpha$ for human, mouse, and chicken proteins. In the C2-Domains, Ca^{2+} binding residues are cyan, DHPC binding residues are yellow; C1P binding residues are beige, and membrane interaction residues are burgundy. In the Catalytic Domains, active site residues are orange, PAPC polar headgroup interacting residues are blue, PAPC acyl chain interacting residues are lavender, PIP2 interacting residues are magenta, and phosphorylation sites are green. Sequence alignment was generated using Clustal W (***Larkin et al., 2007***).

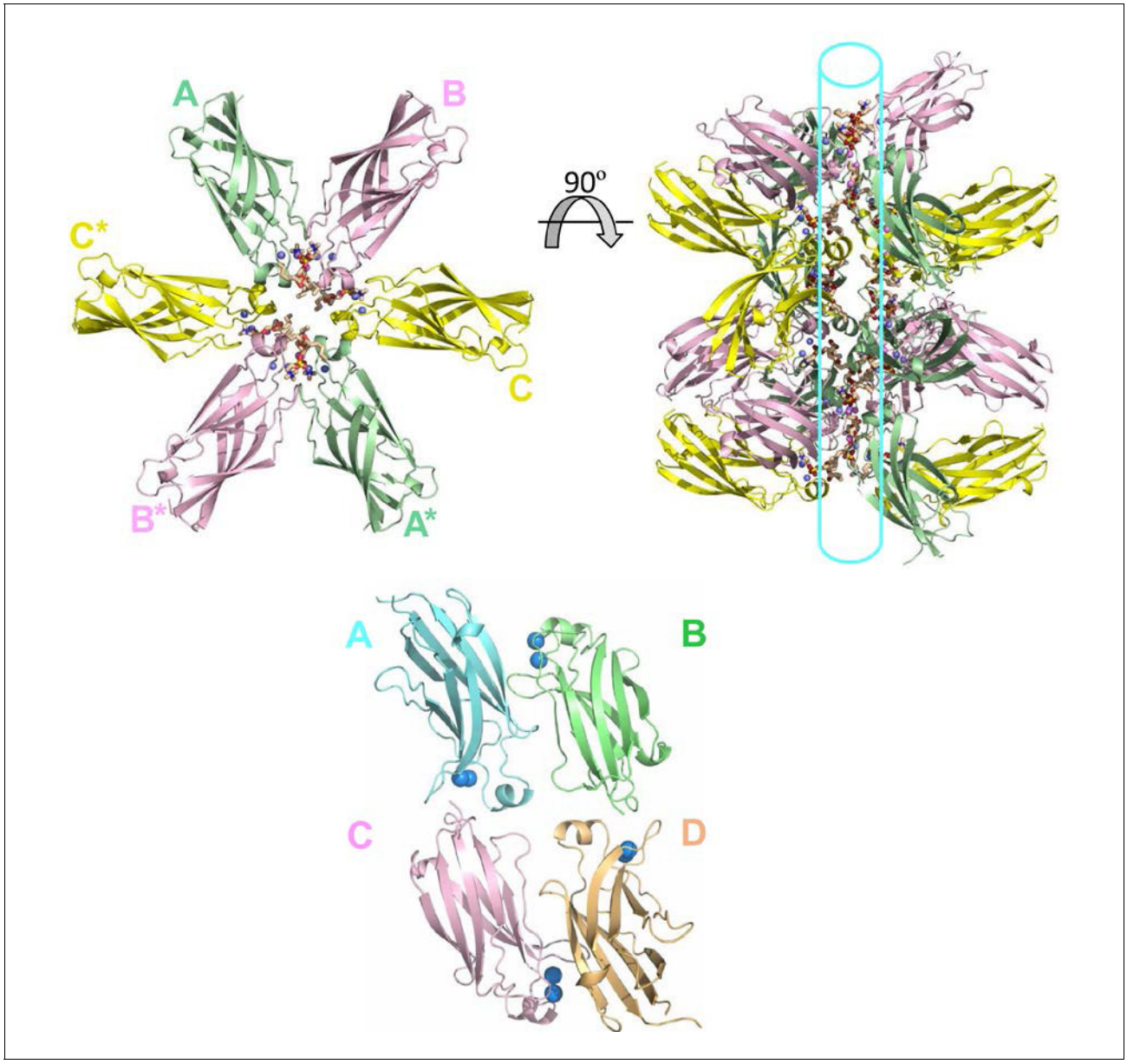

Figure 1—figure supplement 2. Tubular topology formed in the crystal lattice of the cPLA$_2$α C2-domain–DHPC structural complex. (Upper left panel) Cross-sectional view of three cPLA$_2$α C2-PC complexes in the asymmetric unit (labeled A, B, C) and three complexes in the neighboring asymmetric unit (A*, B* and C*) that together form a ring-like structure. The hexanoyl acyl chains associated in one complex are separated from hexanoyl acyl chains in adjacent complexes by 4.9 to 7.2 Å. (Upper right panel) Rotation by 90˚ reveals PC lipids packed into a ring-like topology that forms a tubular-like scaffold. (Lower panel) The crystal packing lattice of lipid-free human cPLA$_2$α C2-domain (PDB: 1RLW). The incorporated Ca^{2+} is shown as blue spheres. Protomer A packs with protomers B and C, but not with protomer D.

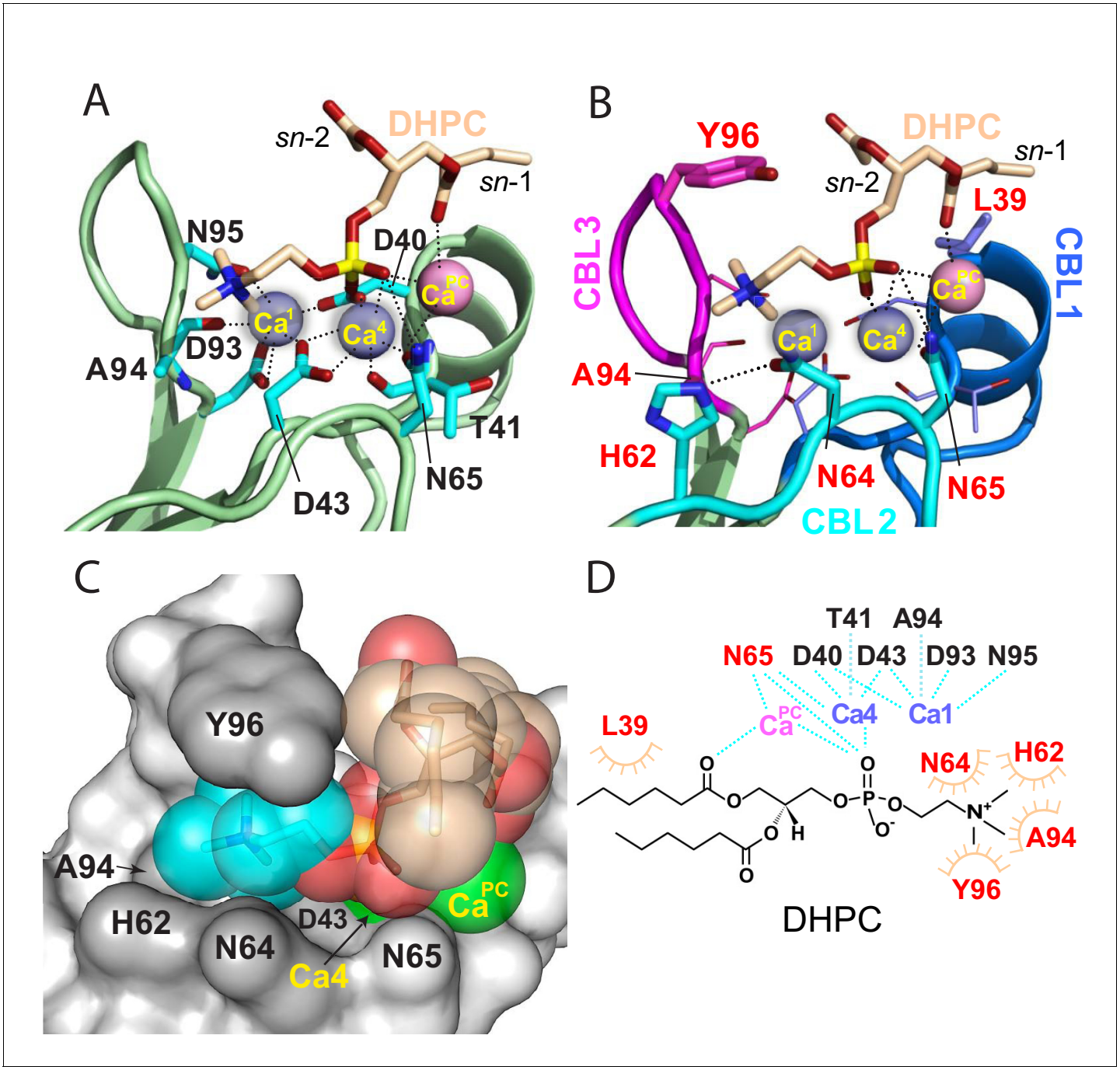

Figure 2. Structural interactions of the cPLA$_2\alpha$ C2-domain complexed with Ca^{2+} and DHPC. (**A**) Coordination of three bound Ca^{2+} ions observed in the C2-domain–DHPC complex. Residues that interact with Ca^{2+} ions are labeled in black with their side-chains (cyan) depicted in a stick representation. (**B**) Same view as in panel (A), but with PC-mediated interactions highlighted. Residues that interact directly with DHPC are labeled in red. (**C**) Space-filling view of bound DHPC and of Ca4 and Ca^{PC} in the cPLA$_2\alpha$ C2-domain. Darker gray residues (Y96, A94, H62, N64, and D43) provide contact surfaces for choline (cyan). Phosphorus is represented in orange; calcium in green; oxygen in red; and acyl carbons in beige. (**D**) Schematic summary of DHPC- and Ca^{2+}-binding interactions with the cPLA$_2\alpha$ C2-domain.

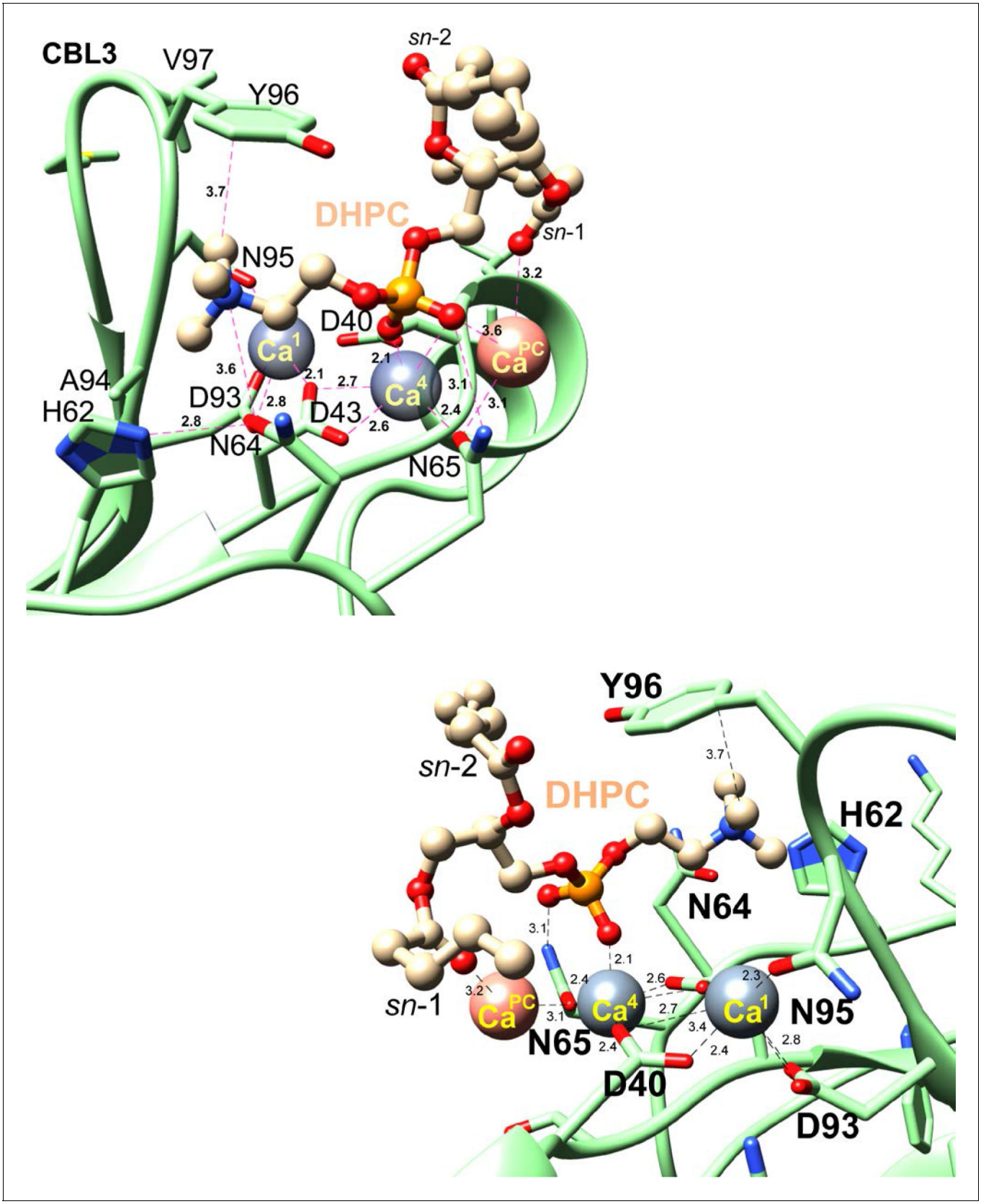
CBL3
V97
Y96
sn-2
DHPC
sn-1
N95
D40
A94
H62
D93
D43
N64
N65
Ca1
Ca4
CaPC
Y96
sn-2
DHPC
H62
N64
sn-1
N65
N95
D40
D93

Figure 2—figure supplement 1. Zoomed views of the cPLA$_2\alpha$ C2-domain complexed with Ca^{2+} and DHPC. C2-domain and DHPC are shown in lime green and beige, respectively. Nitrogen, oxygen, and phosphorus atoms are blue, red, and orange, respectively. Numeric labels for dashed lines equal distances in Ångstroms. Lower structure provides a 'backside' view (relative to the upper structure) by rotation 180˚ in the xy plane.

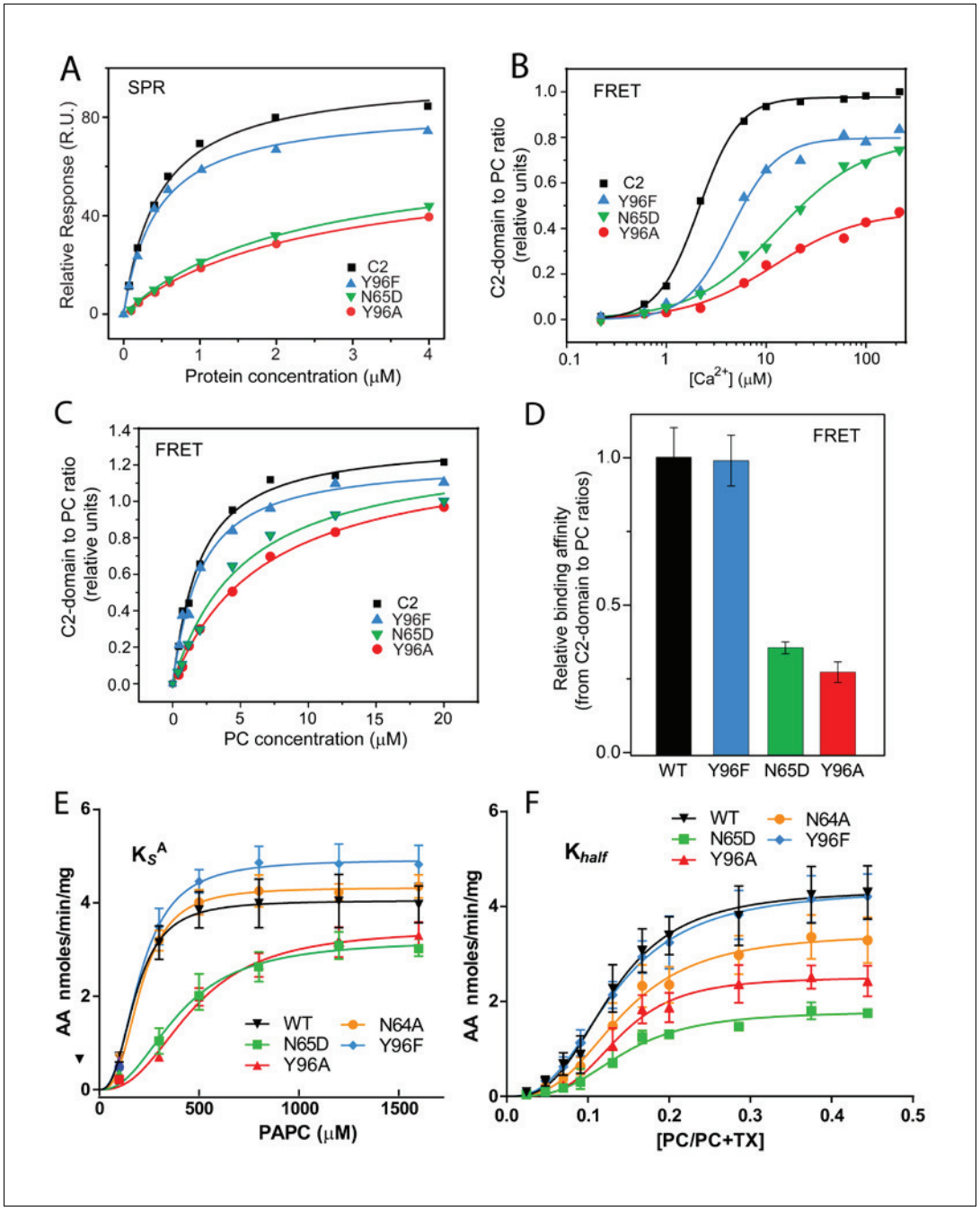

Figure 3. Membrane partitioning of cPLA$_2$α C2-domains and cPLA$_2$α catalytic activities of point-mutated C2-domains in the PC-binding region. (**A**) SPR binding isotherms showing point mutant and control protein equilibrium adsorption to immobilized 1-palmitoyl-2-oleoyl phosphatidylcholine (POPC) vesicles saturating a L1 sensor chip at 5 μl/min solution flow rates (see 'Materials and methods'). (**B**) FRET binding isotherms showing the Ca^{2+} dependence of point mutant and control protein (0.5 μM) equilibrium adsorption to POPC–DHPC bicelle-dilution vesicles (4 μM) (see 'Materials and methods'). (**C**) FRET-binding isotherms showing the POPC–DHPC bicelle-dilution vesicle dependence of point mutant and control protein (0.5 μM) equilibrium adsorption at 50 μM Ca^{2+} (see 'Materials and methods'). (**D**) Relative binding affinity of C2-domain point mutants and control protein obtained for binding isotherms shown in panel (C). (**E**) Effect of the Y96F, Y96A, N64A, and N65D mutations on the dissociation constant (K_s^A) of human cPLA$_2$α activity. Proteins were purified as described ***Stahelin et al. (2007)***. Activity was measured as a function of PC molar concentration for 60 min at 37°C. The PC mole fraction was held constant at 0.285. cPLA$_2$α activities (nmol of arachidonic acid released/min/mg of recombinant cPLA$_2$α) were collected on eight separate occasions and are presented as n = 4 for Y96F, n = 4 for Y96A, n = 4 for N64A,

Figure 3 continued on next page

Figure 3 continued

n = 4 for N65D, and n = 8 for WT. Error = standard deviation. R^2 values are 0.9021, 09609, 0.9586, 0.9780, and 0.9485 for WT, Y96F, Y96A, N64A, and N65D, respectively. (**F**) Effect of Y96F, Y96A, N64A, and N65D mutations on the allosteric sigmoidal constant (K_{half}) of human cPLA$_2\alpha$ activity. Activity was measured as a function of increasing PC mole fractions for 60 min at 37˚C. The PC mole fraction ([PC]/[PC]+[TX-100]) was 0.024 at 50 µM PC, 0.047 at 100 µM PC, 0.069 at 150 µM, 0.091 at 200 µM, 0.13 at 300 µM PC, 0.166 at 400 µM, 0.2 at 500 µM PC, 0.28 at 800 µM PC, 0.37 at 1200 µM PC, and 0.44 at 1600 µM PC. cPLA$_2\alpha$ activities (nmol of arachidonic acid released/min/mg of recombinant cPLA$_2\alpha$) were collected on ten separate occasions and are presented as n = 4 for Y96F, n = 4 for Y96A, n = 4 for N64A, n = 4 for N65D, and n = 4 for WT. Error = standard deviation. R^2 values are 0.9413, 0.9577, 0.9407, 0.9376, and 0.9761 for WT, Y96F, Y96A, N64A, and N65D, respectively.

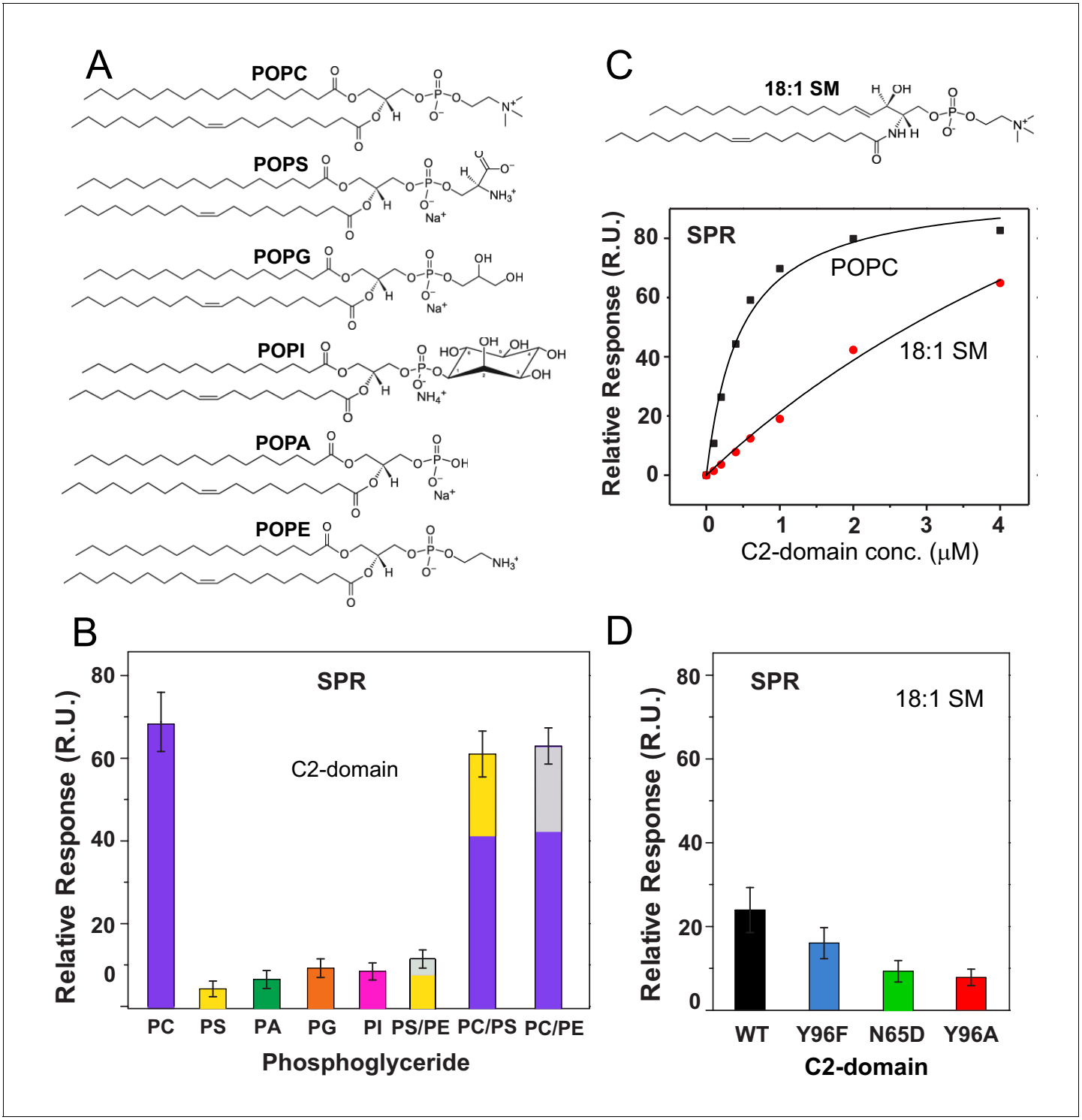

Figure 4. cPLA$_2\alpha$ C2-domain binding affinity for phosphoglyceride and sphingomyelin (SM) vesicles. (**A**) Phosphoglyceride structural formulas. (**B**) Relative affinities of the C2-domain (1 μM) for different phosphoglycerides obtained by SPR. Molar ratios for PS/PE, PC/PS and PC/PE mixed composition vesicles are 7:3. (see ***Figure 4—figure supplement 1***). (**C**) SPR binding isotherms showing C2-domain equilibrium adsorption to immobilized POPC or 18:1-SM vesicles as a function of protein concentration (see ***Figure 4—figure supplement 2*** for additional information). (**D**) Effect of C2-domain mutations (1 μM) on binding to 18:1 SM obtained by SPR (see 'Materials and methods' for other details).

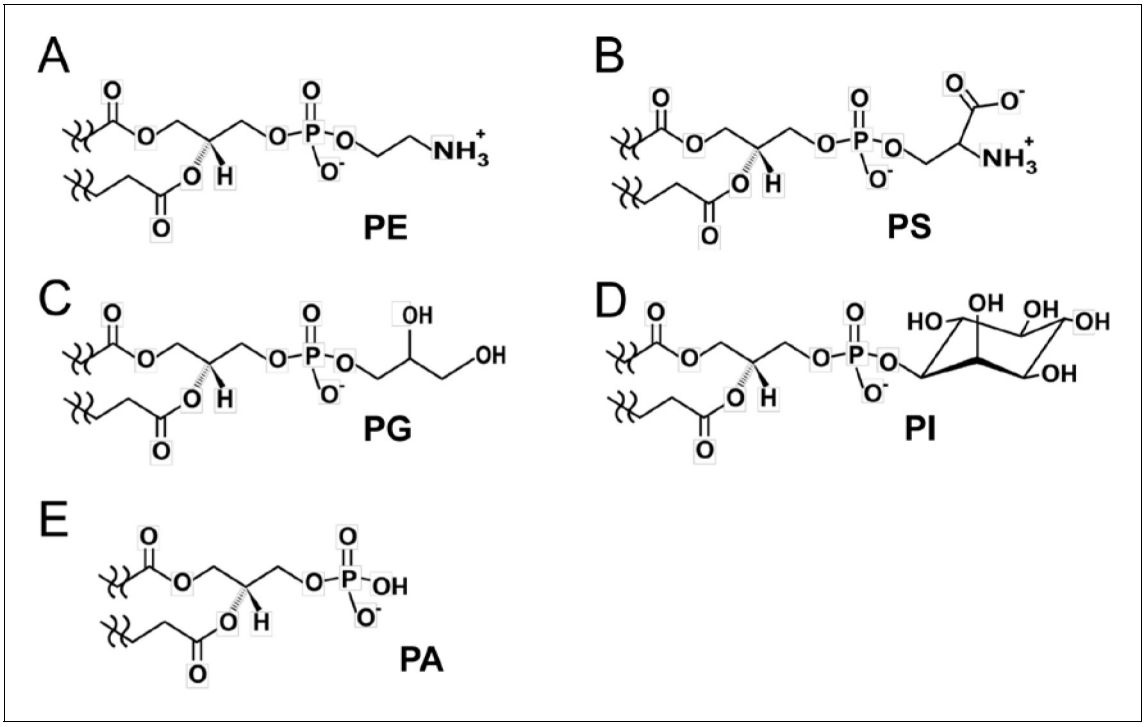

Figure 4—figure supplement 1. Assessment of C2-domain binding to different phosphoglycerides. Head group chemical formulas of various non-PC membrane phosphoglycerides are (**A**) phosphatidylethanolamine, PE; (**B**) phosphatidylserine, PS; (**C**) phosphatidylglycerol, PG; (**D**) phosphatidylinositol, PI; and (**E**) phosphatidic acid, PA. All of the phosphoglycerol-based lipids have the same backbone topology but different head groups that define C2-domain binding specificity. Our findings reveal that the π-cation interaction is critical for binding to PC. PE (**A**) has a primary ammonium group replacing the $-N^{+}(CH_3)_3$ group in PC. Yet, earlier FRET data (***Nalefski et al., 1998***) and our SPR data (***Figure 4B***) indicate relatively weak binding of $cPLA_2\alpha$ C2-domain to PE. The electrostatic potential difference and diminished van der Waals contacts with Ala94, His62, and Asn64 could account for the binding affinity decrease for PE compared to PC. PS has a seryl group (**B**) replacing the $-N^{+}(CH_3)_3$ group in PC. Although the primary ammonium group in the seryl group would seem to be a candidate for undergoing π-cation interaction with Tyr96, binding by C2-domain is weak (***Figure 4B***) suggesting steric clashing of the seryl carboxylate group with CBL residues. PG (**C**) and PI (**D**) are not suitable for interaction with $cPLA_2\alpha$ C2-domain due to lack of an ammonium group and steric clashing by their bulky head groups. PA (**E**) has only a phosphoryl moiety as its head group, which promotes weak interaction. Our SPR binding data showing much weaker binding of these phosphoglyerides compared to PC (***Figure 4B***) are consistent with previous findings obtained using other techniques (***Mosior et al., 1998***; ***Nalefski et al., 1998***; ***Six and Dennis, 2003***).

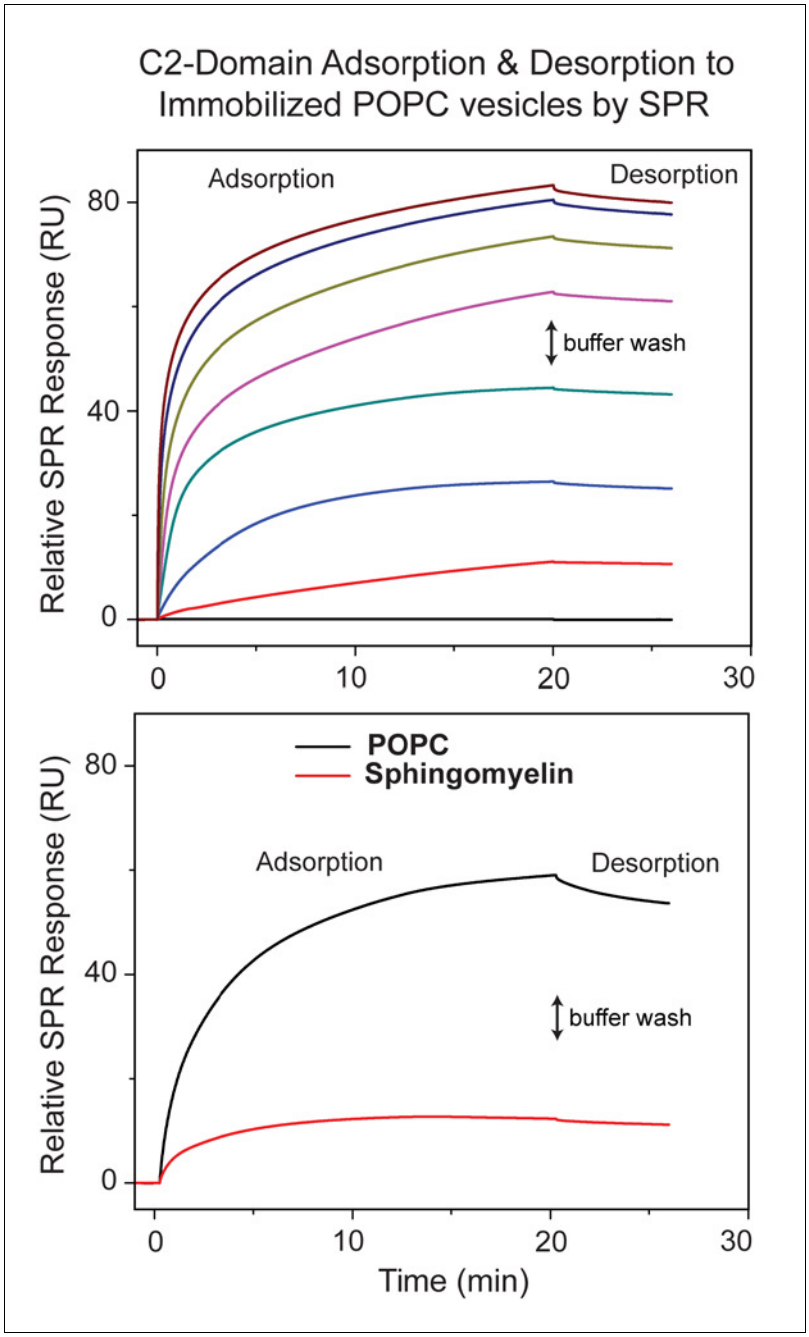

Figure 4—figure supplement 2. The concentration- and time-dependence of C2-domain adsorption/desorption to/from immobilized POPC and 18:1 SM vesicles measured by SPR. (**Upper panel**) SPR data showing cPLA$_2\alpha$ C2-domain adsorption/desorption to/from immobilized POPC vesicles at varying protein concentrations (0.1, 0.2, 0.4, 0.6, 1, 2, and 4 μM; bottom to top) and 5 μl/min flow rate. The two-headed arrow indicates switch to buffer containing no protein. The same approach was used to assess C2-domain adsorption to immobilized 18:1-SM vesicles shown in ***Figure 4C and 4D***. The *Kd* values calculated from the binding isotherms for C2-domain and the point mutants are reported in ***Table 1***. (**Lower panel**) SPR data showing the time-dependence for cPLA$_2\alpha$ C2-domain adsorption/desorption to/from immobilized 18:1 SM vesicles at 0.6 μM protein concentration.

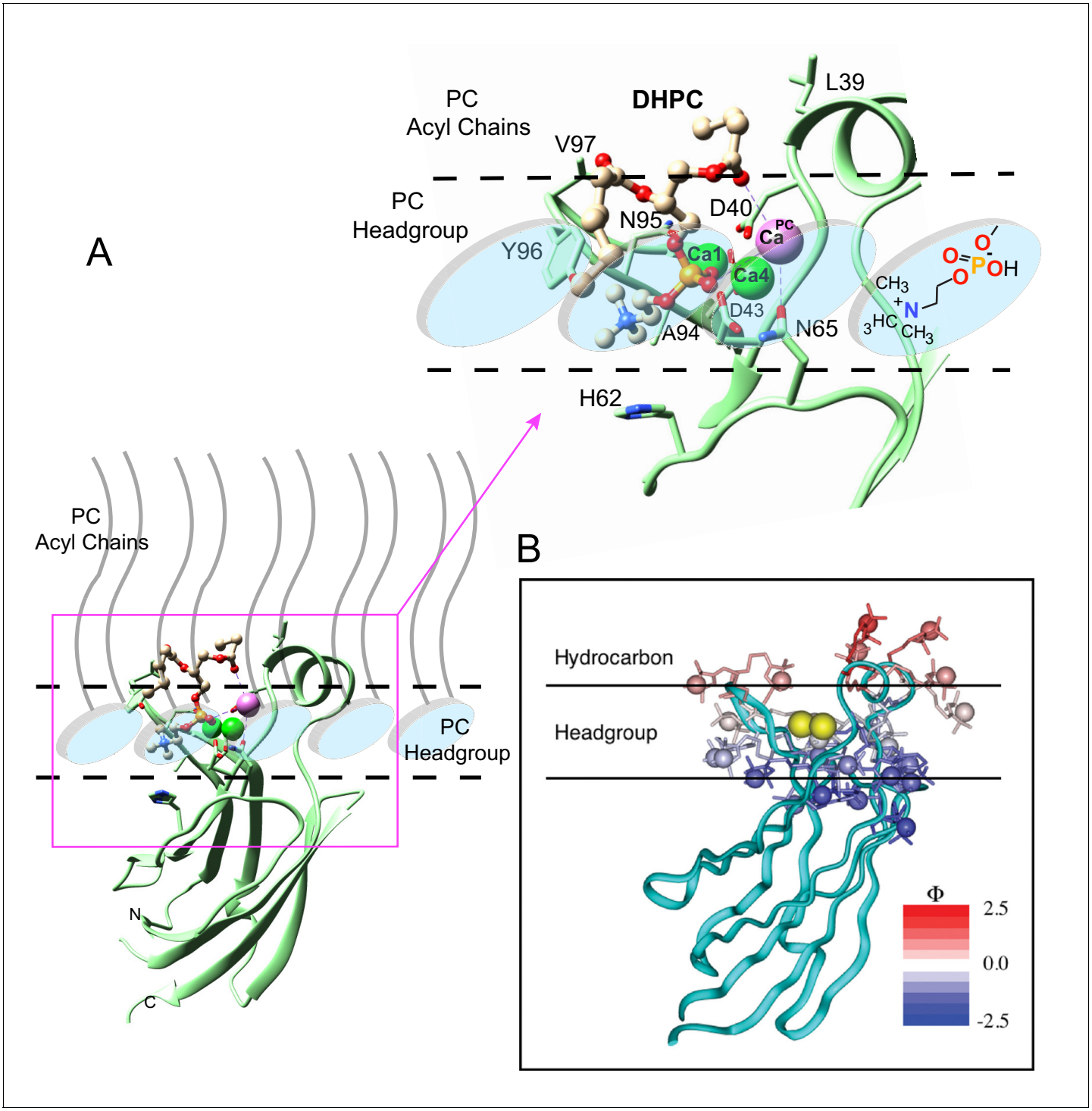

Figure 5. Model of the cPLA$_2\alpha$ C2-domain selectively interacting with the PC membrane interface. (**A**) Interaction of the C2-domain–DHPC structural complex with a PC membrane interface produced by *ad hoc* modeling. The dashed horizontal lines represent planar boundaries for the lipid headgroup and hydrocarbon regions of the PC bilayer. The crystal structure of the C2-domain–DHPC complex is represented as pale green ribbon. The Ca^{2+} ion that is unique to the C2-domain–DHPC complex is shown as a pale magenta sphere; whereas the other two Ca^{2+} ions are shown as green spheres. In the bound DHPC structure, blue, red, orange, and beige colors represent nitrogen, oxygen, phosphorus, and carbon atoms, respectively. The zoomed view shows how the orientation and position of the PC headgroup bound by the C2-domain requires no major conformational change relative to those of unbound PC headgroups comprising the membrane interface. Membrane docking orientation and penetration depth by the C2-domain are based on previous data illustrated in panel (**B**) (***Nalefski and Falke, 1998***; ***Ball et al., 1999***; ***Malmberg et al., 2003***; ***Malmberg and Falke, 2005***). (**B**) cPLA$_2\alpha$ C2-domain docking orientation and penetration depth at the membrane interface, as determined by electron paramagnetic

Figure 5 continued on next page

Figure 5 continued

resonance power saturation. [Reprinted (adapted) with permission ***Malmberg et al., 2003***, Biochemistry 42, 13227–13240. Copyright: American Chemical Society.]. The crystal structure of the lipid-free C2-domain (PDB: RLW) is represented by the cyan ribbon with two Ca^{2+} ions shown as yellow spheres. The horizontal lines represent planar boundaries for the lipid headgroup and hydrocarbon regions of the bilayer. Protein spin labels oriented in their final optimized conformations are colored according to their measured depth parameters (**Φ**), with positive and negative depth parameters indicated by increasing red and blue color intensity, respectively.

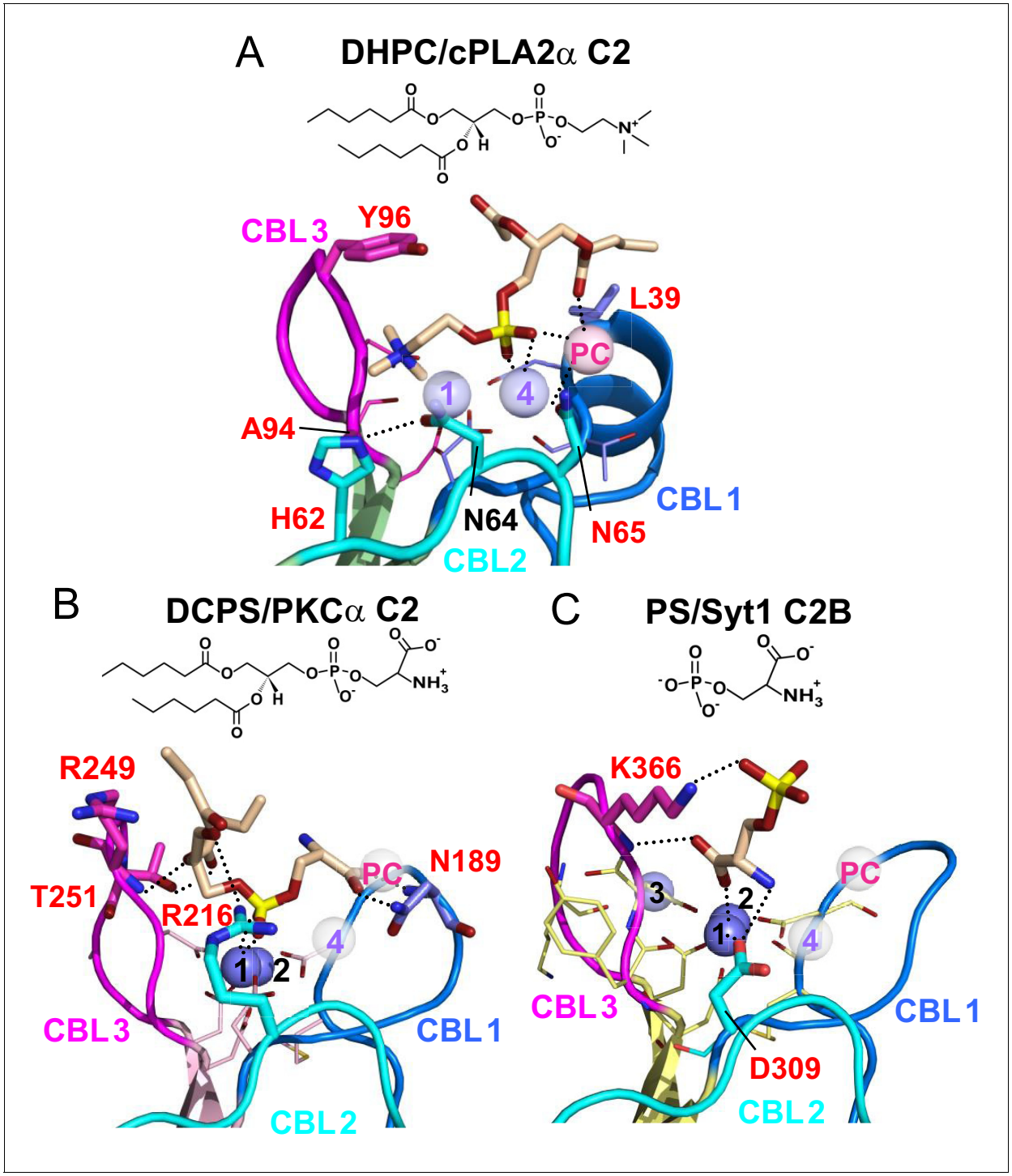

Figure 6. Structures of various C2-domains bound to lipids. (**A**) cPLA$_2$α C2-domain bound to DHPC determined in this study. (**B**) PKCα C2-domain bound to phosphatidylserine (PDB 1DSY). (**C**) Synaptotagmin-1 C2B-domain bound to phosphoserine (PDB 2YOA). For comparison, Ca4 (purple sphere) and Ca^{PC} (pink sphere) in panel (**A**) are overlaid as pale white spheres in panels (**B**) and (**C**). Residues that are interacting directly with ligand are shown as stick models and labeled in red.

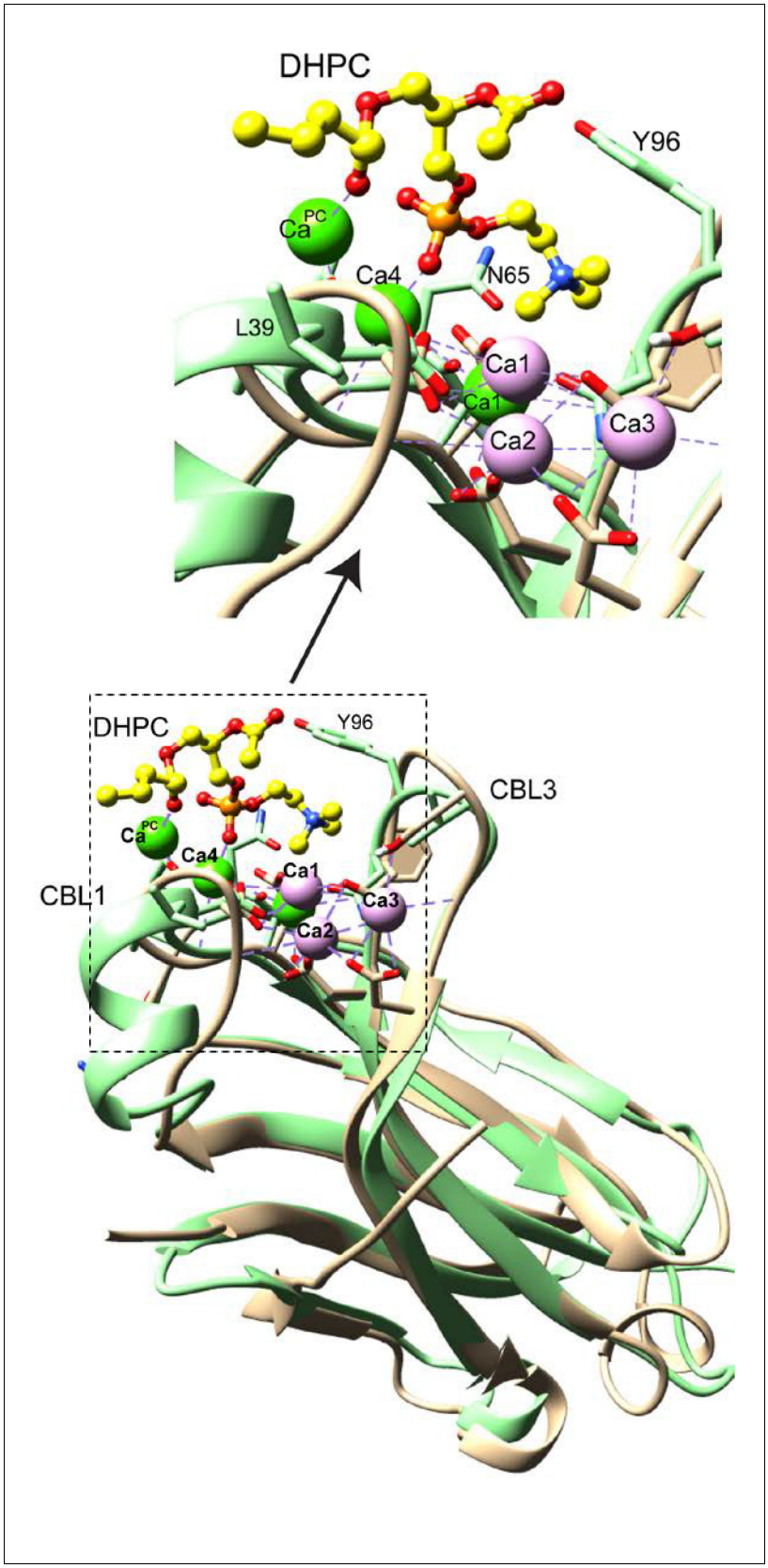

Figure 6—figure supplement 1. Ca^{2+} binding site differences in the synaptotagmin-1 C2A domain versus the $cPLA_2\alpha$ C2-domain complexed with DHPC. $cPLA_2\alpha$ C2-domain complexed with DHPC. $cPLA_2\alpha$ C2-domain

Figure 6—figure supplement 1 continued on next page

Figure 6—figure supplement 1 continued

(green) is shown with bound Ca^{2+} (green) and bound DHPC (yellow). Both Ca4 and Ca^{PC} are directly involved in DHPC binding. Synaptotagin-1 C2A domain (beige) also binds three Ca^{2+} atoms (plum) (PBD:1BYN). Only one Ca^{2+} binding site (Ca1) overlaps with cPLA2 C2-domain. In contrast, all three Ca^{2+} binding positions in synaptotagin-1 C2B domain (***Figure 6C***) overlap with those in synaptotagin-1 C2A. Ca^{2+} binding site identification corresponds with the numbering system of ***Rizo and Südhof (1998)***.

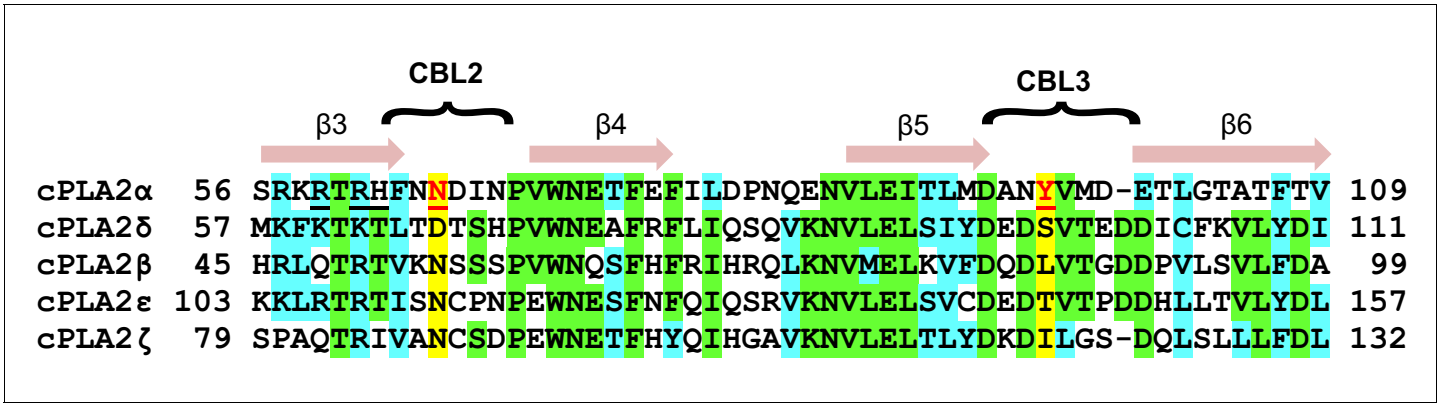

Figure 7. C2-domain sequence alignment for five human cPLA$_2$ isoforms showing the uniqueness of the Tyr96 residue in the cPLA$_2\alpha$ C2-domain. β-strand sequences (arrows) as well as CBL2 and CBL3 sequences (bracketed) are shown above the alignment. Green highlights represent identical residues. Cyan highlights represent similar residues. The yellow highlights facilitate comparison of other isoform residues with N65 and Y96 (red) which are key for PC selectivity by the cPLA$_2\alpha$ C2-domain. Underlined black residues in cPLA$_2\alpha$ (R59, R61, and H62) participate in C1P binding (***Stahelin et al., 2007***; ***Ward et al., 2013***). Sequence alignment was generated using Clustal Omega.